

# Radio QPO in the $\gamma$ -ray-loud X-ray binary LS I +61°303

F. Jaron,<sup>1,2\*</sup> R. Sharma,<sup>1</sup> M. Massi,<sup>1</sup> L. Fuhrmann,<sup>1,3</sup> E. Angelakis,<sup>1</sup> I. Myserlis,<sup>1</sup>  
Guang-Xing Li<sup>4</sup> and Xun Shi<sup>5</sup>

<sup>1</sup>Max-Planck-Institut für Radioastronomie, Auf dem Hügel 69, D-53121 Bonn, Germany

<sup>2</sup>Institut für Geodäsie und Geoinformation – IGG, Universität Bonn, Nußallee 17, D-53115 Bonn, Germany

<sup>3</sup>Universität Siegen, Lehrstuhl für Hochfrequenzsensoren und Radarverfahren, Paul-Bonatz-Str. 9-11 D-57076 Siegen, Germany

<sup>4</sup>Ludwig-Maximilians Universität München, Department für Physik, Scheinerstr. 1, D-81679 München, Germany

<sup>5</sup>Max-Planck-Institut für Astrophysik, Karl-Schwarzschild-Str. 1, D-85748 Garching, Germany

Accepted XXX. Received YYY; in original form ZZZ

## ABSTRACT

LS I +61°303 is a  $\gamma$ -ray emitting X-ray binary with periodic radio outbursts with time scales of one month. Previous observations have revealed microflares superimposed on these large outbursts with periods ranging from a few minutes to hours. This makes LS I +61°303, along with Cyg X-1, the only TeV emitting X-ray binary exhibiting radio microflares. To further investigate these microflaring activity in LS I +61°303 we observed the source with the 100-m Effelsberg radio telescope at 4.85, 8.35, and 10.45 GHz and performed timing analysis on the obtained data. Radio oscillations of 15 hours time scales are detected at all three frequencies. We also compare the spectral index evolution of radio data to that of the photon index of GeV data observed by *Fermi*-LAT. We conclude that the observed QPO could result from multiple shocks in a jet.

**Key words:** Radio continuum: stars – X-rays: binaries – X-rays: individual (LS I +61°303)

## 1 INTRODUCTION

It is a known fact that a subclass of X-ray binaries and a subclass of Active Galactic Nuclei (AGN) are sources of radio emission. There is evidence that radio outbursts in these systems are superimposed by microflaring activity of lower amplitude and short time scales. These short timescale variations, characterised as Quasi-Periodic Oscillations (QPO) (Fender et al. 1997), may change period between different epochs or are present in a relatively short interval of time, with few oscillations. In X-ray binaries with radio jets, i.e., microquasars (Mirabel & Rodríguez 1999), QPO were first observed in the black hole system V404 Cyg where a range of 22–120 min sinusoidal radio variations were observed during the decay of a radio outburst (Han & Hjellming 1992), and more recently Plotkin et al. (2017) found correlation between radio and X-ray variability on minute time scales. Short-term radio variability on time scales of  $\sim 1$  hour was observed in Cyg X-1 (Marti et al. 2001). QPO in GRS 1915+105 have been extensively studied, e.g., by Pooley & Fender (1997), who revealed QPO with periods in the range of 20–40 min; observations by Rodríguez & Mirabel (1997) showed oscillations of 30 min. Also, Fender et al. (2002) performed an analysis at dual radio frequencies and again revealed QPO with periods of  $\sim 30$  min following the decay of a major outburst. More-

over, the radio spectral index  $\alpha$  oscillates from negative to positive values (see Fig. 2 in Fender et al. 2002). Fender & Pooley (1998) demonstrated that infrared oscillations precede the radio ones, and both oscillations have similar period and shape. In simultaneous radio and X-ray observations of GRS 1915+105, Klein-Wolt et al. (2002) showed that X-ray dips were associated with radio peaks. Oscillations with time scales of days are known to occur in Cyg X-3 (Zimmermann et al. 2015). These longer period QPO are present in both total flux density and radio spectral index (Fig. 1).

QPO seem to be a general phenomenon associated to the ejections in accreting systems and have in fact been observed also in AGN. X-ray QPO of 55 minutes have been indicated in the flat spectrum radio quasar 3C 273 (Espaillat et al. 2008) and QPO of  $\sim 60$  minutes have been observed in the narrow-line Seyfert 1 Galaxy RE J1034+396 (Gierliński et al. 2008). Rani et al. (2010) found evidence for optical QPO of 15 minutes in the blazar S5 0716+714 in R-band.

The physical process behind QPO is still a matter of debate, three explanations are discussed. The first hypothesis explains QPO as the result of a single shock propagating down a helical jet and producing increased flux each time the shock meets another twist of the helix at the angle that provides the maximum Doppler boosting for the observer (Rani et al. 2010). In the second scenario, QPO could be related to shocks passing down the jet and accelerating particles in situ (Klein-Wolt et al. 2002, and references therein).

\* E-mail: fjaron@mpifr-bonn.mpg.de

As a third explanation, QPO have been related to discrete ejections of plasma. Multi-wavelength QPO observations of GRS 1915+105 (see references in [Mirabel & Rodríguez 1999](#)) have been interpreted as periodic discrete ejections of plasma, with a mass of about  $\sim 10^{19}$  g and at relativistic speeds, with subsequent replenishment of the inner accretion disk.

Testing possible models for the origin of QPO is still complicated because of insufficient statistics. Remaining open questions include: How stable are these “quasi” periodic oscillations? Why are QPO present in the radio spectral index? Why does the radio spectrum oscillate between optically thin and thick emission in GRS 1915+105 and Cyg X-3, and is that a general property of QPO? Do the “flat” radio spectra in microquasars and AGN indeed arise from the combination of emission from optically thick and thin regions as suggested in [Fender et al. \(2002\)](#)? In order to answer these questions, it is requisite to increase the sample of X-ray binaries exhibiting radio QPO. For this purpose we investigate on LS I +61°303 which is one of the few radio emitting X-ray binaries which also emits in  $\gamma$ -rays (GeV, [Abdo et al. 2009](#), and TeV, [Albert et al. 2006](#), [Acciari et al. 2008](#)). Moreover, LS I +61°303 is periodic at all wavelengths on the orbital time scale (26.5 d) and has revealed microflaring activity (Sect. 2).

Aimed at investigating QPO in LS I +61°303 we performed new observations with the Effelsberg 100-m radio telescope. Our new radio observations and data analysis are described in Sect. 3 along with the description of *Fermi*-LAT data reduction. In Sect. 4 we present our results and in Sect. 5 our conclusions.

## 2 THE BINARY SYSTEM LS I +61°303

The X-ray binary LS I +61°303 is composed of a Be star ([Casares et al. 2005](#)) and a black hole ([Massi et al. 2017](#)), exhibiting radio outbursts ([Gregory 2002](#); [Jaron & Massi 2013](#)) occurring periodic, related to the orbital period of  $\sim 26.5$  days. With an SED peaking above 1 GeV, LS I +61°303 can further be classified as a  $\gamma$ -ray binary (see Table 2 in [Dubus 2013](#)). Among the black hole binaries discussed above, only LS I +61°303 and Cyg X-1 have the peculiarity of emitting at TeV, this, however, being a transient phenomenon for Cyg X-1 ([Albert et al. 2006](#)), and also LS I +61°303 has episodes of TeV non-detection ([Acciari et al. 2011](#)).

Two magnetar-like signals were detected from a large region of sky crowded by other potential sources beside LS I +61°303 ([Rea & Torres 2008](#)). On that basis [Torres et al. \(2012\)](#) put forward their working hypothesis that LS I +61°303 could be the first magnetar detected in a binary system, and studied the implications. In the magnetar scenario, as well as for the pulsar scenario (see, e.g., [Dubus 2013](#)), variability of the Be star would trigger and explain observed long-term variability in the emission of LS I +61°303 at all wavelengths ([Gregory 2002](#); [Li et al. 2014](#); [Ackermann et al. 2013](#); [Ahnen et al. 2016](#)). However, following the well-studied (i.e., over 100 years) case of the binary system  $\zeta$  Tau, i.e., also a Be star in a binary system (Sect. 4 in [Massi & Torricelli-Ciamponi 2016](#) and references therein), Be star variations last 2-3 cycles only and are of different lengths ([Rivinius et al. 2013](#)). Timing analysis of 37 years of radio data performed by [Massi & Torricelli-Ciamponi \(2016\)](#) reveals that LS I +61°303 does not show merely 2-3 cycles which are of different lengths but a repetition of 8 full cycles of an identical length of 1628 days, well in agreement with the scenario of a microquasar with a precessing jet ([Massi & Torricelli-Ciamponi 2014](#); [Jaron et al. 2016](#)). In addition, as discussed in [Jaron et al. \(2016\)](#), the orbital shift in the equivalent width of the

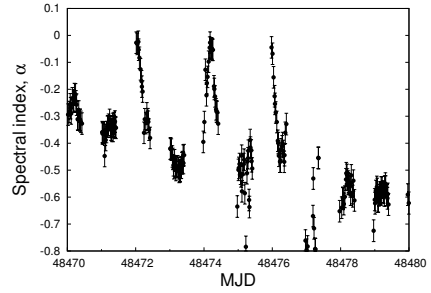


**Figure 1.** Spectral index of Cyg X-3 from Green Bank Interferometer data at 2 and 8 GHz. Three oscillations separated by 3 days are evident. Similar oscillations are present in the flux density at the two frequencies (see [Zimmermann et al. 2015](#)).

H $\alpha$  emission line ([Paredes-Fortuny et al. 2015](#)), points to variations caused by a precessing jet.

Optical polarization observations determined a rotational axis for the Be star of 25 degrees ([Nagae et al. 2008](#)). For parallel orbital and Be spin axes and the mass function determined through orbital motions measurements ([Casares et al. 2005](#)) a 25 degree inclination implies a black hole of 4 solar masses, as argued by [Massi et al. \(2017\)](#), and references therein), who further probe from X-ray observations that the photon index vs. luminosity trend of LS I +61°303 is very different from that of the non-accreting pulsar binary PSR B1259-63, whereas its trend agrees with that of moderate-luminosity regime black holes in general and with the two black holes in the same X-ray luminosity range: Swift J1357.2-0933 and V404 Cygni, in particular.

The source is well-known for its strong radio outbursts with orbital periodicity monitored for  $\sim 40$  years ([Massi & Torricelli-Ciamponi 2016](#)). Along with this strong radio outburst there is also evidence of occurrence of microflaring activity with time scales of minutes to hours. During the decaying phase of one of the radio outbursts of LS I +61°303, a step-like pattern was observed for the first time with the Westerbork Synthesis Radio Telescope (WSRT) with a characteristic timescale of  $\sim 10^3$  s ([Taylor et al. 1992](#)). [Peracaula et al. \(1997\)](#) performed the first systematic study of this short-term radio variability and found a period of 1.4 hours for these microflares with an amplitude of  $\sim 4$  mJy in VLA observations related to the decay of one radio outburst. Recently, [Zimmermann et al. \(2015\)](#) observed during the decay of one outburst of LS I +61°303 sub-flares with a characteristic time-scale of two days (see their Fig. 1). Furthermore, the radio spectral index oscillated in a quasi-regular fashion and the local peaks in spectral index roughly coincide with the peaks of the sub-flares seen in the total intensity light curves. Finally, at higher energy, [Harrison et al. \(2000\)](#) discovered a periodicity of  $\sim 40$  minutes in an X-ray ASCA observation associated to the onset of a radio outburst.

## 3 OBSERVATION AND DATA ANALYSIS

### 3.1 Effelsberg radio telescope

Our multi-frequency flux density measurements were performed about every 45 minutes for almost 100 hours on April 17–21, 2014 (MJD 56764.726 until MJD 56768.763). The orbital phase  $\Phi$  is defined as  $\Phi = \frac{t - t_0}{P_{\text{orb}}} - \text{int}\left(\frac{t - t_0}{P_{\text{orb}}}\right)$ , where,  $t_0 = \text{MJD } 43366.275$ , orbital period  $P_{\text{orb}} = 26.4960 \pm 0.0028$  d ([Gregory 2002](#)), giv-

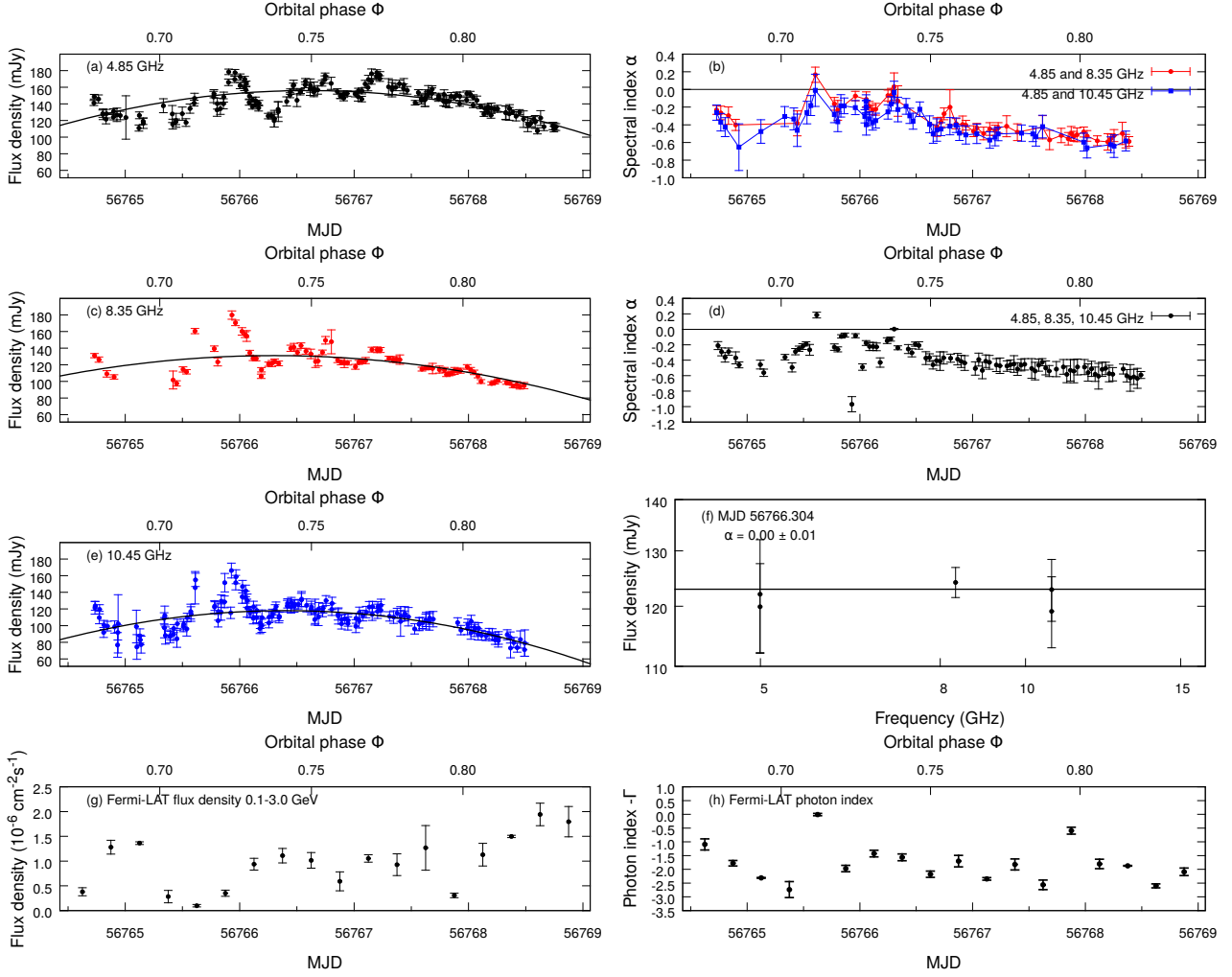


**Figure 2.** (a), (c), (e): Original light curves at indicated frequencies. The light curves were fitted with a parabola (black solid line) in order to remove the long-term trend. (b) Spectral index between indicated frequencies. (d): Spectral index resulting from fitting a power law to all three frequencies. (f): Zoom-in of the flat spectral index at MJD 56766.304, axes in logarithmic scale. (g): *Fermi*-LAT light curve. (h): *Fermi*-LAT photon index.

**Table 1.** Best-fit parameters of the parabola used for subtracting the long-term trend from the lightcurves.

Frequency	$a_1$	$t_0$ (MJD)	$b_1$
4.85 GHz	$-0.009 \pm 0.001$	$56766.6 \pm 0.1$	$0.16 \pm 0.02$
8.35 GHz	$-0.008 \pm 0.001$	$56766.3 \pm 0.1$	$0.13 \pm 0.05$
10.45 GHz	$-0.009 \pm 0.001$	$56766.4 \pm 0.1$	$0.12 \pm 0.03$

ing  $\Phi = 0.68 - 0.83$  for our observations. The secondary focus receivers of the Effelsberg 100-m telescope were used at three frequencies, namely 4.85, 8.35, and 10.45 GHz (6.0, 3.6, 2.8 cm wavelengths respectively). Flux density measurements were performed using the “cross-scan” technique, i.e., progressively slewing over the source position in azimuthal and elevation direction with the number of sub-scans matching the source brightness at a given frequency (typically 4 to 12). At 4.85 and 10.45 GHz, the “beam switch”, realised through multiple-feed systems, removed most of the tropospheric variations, allowing for more accurate measurements. The cross-scan technique on the other hand allows instantaneous correction of small, remaining pointing offsets. The

data reduction, from raw telescope data to calibrated flux densities/spectra, was done in the standard manner as described in Angelakis et al. (2015). Problems with the 8.35 GHz receiver caused the large flagging of data at this frequency. The best data set for sampling rate and SNR is that at 4.85 GHz. The light curves obtained for all three frequencies are shown in Figure 2 (a, c, e) along with their spectral index computed as  $\alpha = \log(S_1/S_2)/\log(\nu_1/\nu_2)$  for Fig 2 b, and as a linear fit to the fluxes vs. frequency in double logarithmic scale for every time bin of 45 minutes, shown in Fig. 2 d.

In order to analyse short-term periodicities, we removed the long-term trend from the light curves by subtracting a quadratic function

$$f_1(t) = a_1(t - t_0)^2 + b_1, \quad (1)$$

with best-fit parameters listed in Table 1. The rectified data were then analyzed using wavelet analysis (Torrence & Compo 1998), auto-correlation function and Lomb-Scargle periodogram (Lomb 1976; Scargle 1982). We test the significance of found periodic signals by employing the Fisher randomisation test (Linnell Nemeč & Nemeč 1985) where the flux is permuted a thousand times

**Table 2.** Best-fit parameters as a result of fitting a sine function to the folded data with period of 15.4 h.

Frequency (Ghz)	$A$ (mJy)	$B$ (mJy)	$\phi_0$	$\chi^2$
4.85	$9.3 \pm 1.2$	$-0.2 \pm 0.8$	$0.7 \pm 0.1$	0.9
8.35	$8.9 \pm 0.9$	$2.1 \pm 0.8$	$0.7 \pm 0.1$	0.8
10.45	$6.7 \pm 0.7$	$0.5 \pm 0.6$	$0.7 \pm 0.1$	1.3

and thousand new randomised time series are created and their periodograms calculated. The proportion of randomised time series that contain a higher peak in the periodogram than the original periodogram at any frequency then gives the false alarm probability  $p$  of the peak. If  $p < 0.01$ , the period is significant, and if  $0.01 < p < 0.1$  the period is marginally significant. The data were then folded on the resulting significant period, and the folded data were fitted with a sine-function

$$f_2(\phi) = A \sin 2\pi(\phi - \phi_0) + B, \quad (2)$$

with its best-fit parameters in Table 2.

### 3.2 Fermi-LAT data reduction

We compare our radio data with GeV  $\gamma$ -ray data. For this purpose we use the GeV data from the *Fermi*-LAT in the energy range 0.1–3.0 GeV from MJD 56764.125 until MJD 56768.875. For the analysis of *Fermi*-LAT data we used version v10r0p5 of the *Fermi* ScienceTools<sup>1</sup>. We used the instrument response function P8R2\_SOURCE\_V6 and the corresponding model gll\_iem\_v06.fits for the Galactic diffuse emission and the template iso\_P8R2\_SOURCE\_V6\_v06.txt. Model files were created automatically with the script make3FGLxml.py<sup>2</sup> from the third *Fermi*-LAT point source catalog (Acero et al. 2015). The spectral shape of LS I +61°303 in the GeV regime is a power law with an exponential cut-off at 4–6 GeV (Abdo et al. 2009; Hadasch et al. 2012). Here we restrict our analysis to the power law part of the GeV emission by fitting the source with

$$\frac{dn}{dE} = n_0 \left( \frac{E}{E_0} \right)^{-\Gamma} \left[ \frac{\text{counts}}{\text{cm}^2 \text{sec dE}} \right] \quad (3)$$

with all parameters left free for the fit, and including data in the energy range  $E = 0.1 - 3$  GeV. All other sources within a radius of  $10^\circ$  and the Galactic diffuse emission were left free for the fit. All sources between  $10^\circ - 15^\circ$  were fixed to their catalog values. The light curves were computed performing this fit for every time bin of width half a day for data from 2014 April 17 (MJD 56764.125) till 2014 April 21 (MJD 56768.875). On average, the test statistic for LS I +61°303 was 40, which corresponds to a detection of the source at the  $6.3\sigma$  level on average in each time bin.

## 4 RESULTS

The light curves at all three frequencies (Fig. 2 a, c, e) show small-scale oscillations. Amplitude and width seem to vary from one peak to the other. The higher sensitivity of 4.85 GHz data give rise to significant timing analysis results: the wavelet analysis in the top panel

<sup>1</sup> available from <http://fermi.gsfc.nasa.gov/ssc/data/analysis/software/>

<sup>2</sup> available from <http://fermi.gsfc.nasa.gov/ssc/data/analysis/user/>

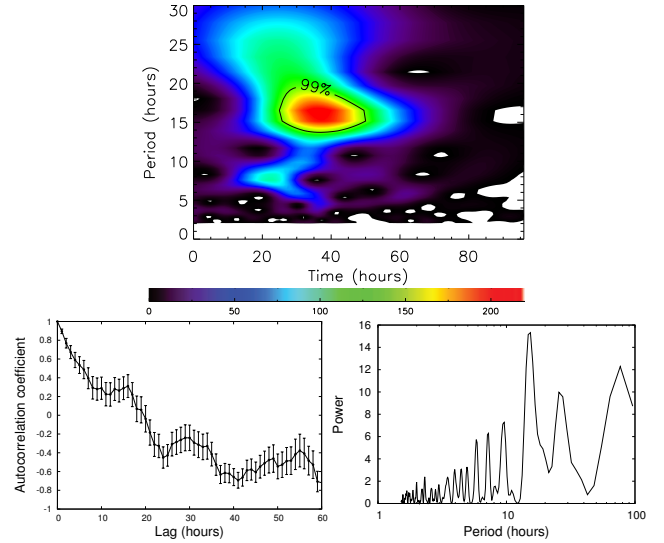


**Figure 3.** Timing analysis results of the 4.85 GHz data. Top: Wavelet plot with maximum power (red) around 16 hours, at the 99 per cent confidence level. Bottom left: Auto-correlation function. Bottom right: Lomb-Scargle periodogram with most significant peak at 15.4 hours.

of Fig. 3 shows that the oscillations at 4.85 GHz have a periodicity of about 16 hours. The auto-correlation coefficient in the middle panel of Fig. 3 shows peaks at 15 hours, 30 hours and at about 55 hours. Lomb-Scargle analysis in the bottom panel of Figure 3 gives a dominant and significant feature at  $15.4 \pm 0.6$  h. Indeed, data at all three frequencies fold with the 15.4 hours period (see Fig. 4 and fitting parameters in Table 2) with significance of the oscillations clearly above  $8\sigma$ . Oscillations are also present in the radio spectral index  $\alpha$  (Fig. 2 d) corroborating the observed spectral index oscillations by Zimmermann et al. (2015, see the bottom panel of their Fig. 1). The oscillations create a sort of flattening of the spectral index, and a zoom-in centered at MJD 56766.3 clearly shows  $\alpha = 0$  (Fig. 2 f).

## 5 CONCLUSIONS AND DISCUSSION

We observed one radio outburst of LS I +61°303 with the Effelsberg 100-m telescope in April 2014 for approximately 100 h at 4.85, 8.35, and 10.45 GHz. We analysed these data along with simultaneous *Fermi*-LAT GeV data. Our results reveal the following:

(i) QPO previously observed in LS I +61°303 showed time scales of minutes, hours and days (Taylor et al. 1992; Peracaula et al. 1997; Zimmermann et al. 2015). Our study determines periodicities of  $\sim 15$  h. There are three hypotheses to explain the physical mechanism behind the occurrence of these periodicities. The first is associated to the geometry of the jet (Rani et al. 2010), the second one to multiple shocks (Klein-Wolt et al. 2002, and references therein), and the third one implies discrete plasma ejections (Mirabel & Rodríguez 1999, and references therein). In the first scenario the reason for oscillations is the helical topology of the magnetic field in the jet associated to Doppler boosting effects. Since in a conical jet of a microquasar the 10 GHz emission originates from a jet-segment nearer to the central engine of the system than the 5 GHz jet-segment (Kaiser 2006), this scenario implies a longer period for 5 GHz oscillations. This is not compatible with



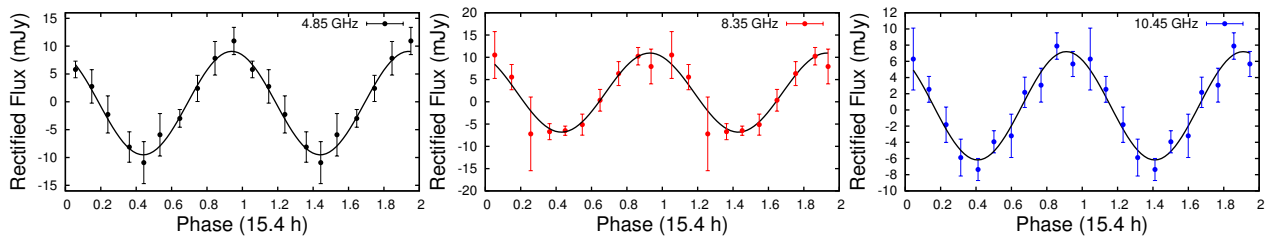


**Figure 4.** Rectified flux folded on the period of 15.4 h, which resulted most significant from timing analysis. Error bars reflect the  $1\sigma$  uncertainties resulting from the standard deviation in each phase bin. The data are repeated in the second cycle. The solid line (black) is a result of fitting a sine function to the folded data. The data are taken from the time-intervals: 4.85 GHz, MJD 56765.64 – 56768.48 (4.4 cycles); 8.35 GHz, MJD 56766.06 – 56767.64 (2.5 cycles); 10.45 GHz, MJD 56765.98 – 56768.48 (3.9 cycles).

our results in Table 2 and Fig. 4, giving the same period for the oscillations at all three observed frequencies. Following the Van der Laan (1966) model of adiabatically expanding spheroidal ejecta of plasma, the low-frequency emission peak is delayed and weaker than that at higher frequencies. Our result of a larger amplitude at lower frequency is in contradiction with this model. Finally, the shock-in-jet model proposed by Marscher & Gear (1985) and generalised by Valtaoja et al. (1992) predicts flare amplitudes to increase towards lower frequency, as observed.

(ii) As previously observed in X-ray binaries GRS 1915+105 and Cyg X-3, the radio spectral index of LS I +61°303 oscillates in phase with total flux variations, the radio spectral index modulation being superimposed on a longer modulation whose peak corresponds to the flattening of the spectral index. This finding is consistent with the hypothesis that the “flat” radio spectra in microquasars arise from the combination of emission from optically thick and thin regions (Fender et al. 2002). The radio spectrum after the oscillations becomes optically thin with  $p \sim 2.0$ , the  $\gamma$ -ray emission follows a similar trend with a photon index  $\Gamma \sim 2.0$ .

## ACKNOWLEDGEMENTS

We thank Eduardo Ros for carefully reading the manuscript. This work has made use of public *Fermi* data obtained from the High Energy Astrophysics Science Archive Research Center (HEASARC), provided by NASA Goddard Space Flight Center.

## REFERENCES

- Abdo A. A., et al., 2009, *ApJ*, 701, L123  
 Acciari V. A., et al., 2008, *ApJ*, 679, 1427  
 Acciari V. A., et al., 2011, *ApJ*, 738, 3  
 Acero F., et al., 2015, *ApJS*, 218, 23  
 Ackermann M., et al., 2013, *ApJ*, 773, L35  
 Ahnen M. L., et al., 2016, *A&A*, 591, A76  
 Albert J., et al., 2006, *Science*, 312, 1771  
 Angelakis E., et al., 2015, *A&A*, 575, A55  
 Casares J., Ribas I., Paredes J. M., Martí J., Allende Prieto C., 2005, *MNRAS*, 360, 1105  
 Dubus G., 2013, *A&ARv*, 21, 64  
 Espaillat C., Bregman J., Hughes P., Lloyd-Davies E., 2008, *ApJ*, 679, 182  
 Fender R. P., Pooley G. G., 1998, *MNRAS*, 300, 573  
 Fender R. P., Pooley G. G., Robinson C. R., Harmon B. A., Zhang S. N., Canosa C., 1997, in Wickramasinghe D. T., Bicknell G. V., Ferrario L., eds, *Astronomical Society of the Pacific Conference Series Vol. 121, IAU Colloq. 163: Accretion Phenomena and Related Outflows*. p. 701 ([arXiv:astro-ph/9612092](https://arxiv.org/abs/astro-ph/9612092))  
 Fender R. P., Rayner D., Trushkin S. A., O’Brien K., Sault R. J., Pooley G. G., Norris R. P., 2002, *MNRAS*, 330, 212  
 Gierliński M., Middleton M., Ward M., Done C., 2008, *Nature*, 455, 369  
 Gregory P. C., 2002, *ApJ*, 575, 427  
 Hadasch D., et al., 2012, *ApJ*, 749, 54  
 Han X., Hjellming R. M., 1992, *ApJ*, 400, 304  
 Harrison F. A., Ray P. S., Leahy D. A., Waltman E. B., Pooley G. G., 2000, *ApJ*, 528, 454  
 Jaron F., Massi M., 2013, *A&A*, 559, A129  
 Jaron F., Torricelli-Ciamponi G., Massi M., 2016, *A&A*, 595, A92  
 Kaiser C. R., 2006, *MNRAS*, 367, 1083  
 Klein-Wolt M., Fender R. P., Pooley G. G., Belloni T., Migliari S., Morgan E. H., van der Klis M., 2002, *MNRAS*, 331, 745  
 Li J., Torres D. F., Zhang S., 2014, *ApJ*, 785, L19  
 Linnell Nemeč A. F., Nemeč J. M., 1985, *AJ*, 90, 2317  
 Lomb N. R., 1976, *Ap&SS*, 39, 447  
 Marscher A. P., Gear W. K., 1985, *ApJ*, 298, 114  
 Martí J., Mirabel I. F., Rodríguez L. F., 2001, *Information Bulletin on Variable Stars*, 5127  
 Massi M., Torricelli-Ciamponi G., 2014, *A&A*, 564, A23  
 Massi M., Torricelli-Ciamponi G., 2016, *A&A*, 585, A123  
 Massi M., Migliari S., Chernyakova M., 2017, preprint, ([arXiv:1704.01335](https://arxiv.org/abs/1704.01335))  
 Mirabel I. F., Rodríguez L. F., 1999, *ARA&A*, 37, 409  
 Nagae O., Kawabata K. S., Fukazawa Y., Okazaki A., Isogai M., 2008, in Yuan Y.-F., Li X.-D., Lai D., eds, *American Institute of Physics Conference Series Vol. 968, Astrophysics of Compact Objects*. pp 328–330, doi:10.1063/1.2840421  
 Paredes-Fortuny X., Ribó M., Bosch-Ramon V., Casares J., Fors O., Núñez J., 2015, *A&A*, 575, L6  
 Peracaula M., Martí J., Paredes J. M., 1997, *A&A*, 328, 283  
 Plotkin R. M., et al., 2017, *ApJ*, 834, 104  
 Pooley G. G., Fender R. P., 1997, *MNRAS*, 292, 925  
 Rani B., Gupta A. C., Joshi U. C., Ganesh S., Wiita P. J., 2010, *ApJ*, 719, L153  
 Rea N., Torres D. F., 2008, *The Astronomer’s Telegram*, 1731  
 Rivinius T., Carciofi A. C., Martayan C., 2013, *A&ARv*, 21, 69  
 Rodríguez L. F., Mirabel I. F., 1997, *ApJ*, 474, L123  
 Scargle J. D., 1982, *ApJ*, 263, 835  
 Taylor A. R., Kenny H. T., Spencer R. E., Tzioumis A., 1992, *ApJ*, 395, 268  
 Torrence C., Compo G. P., 1998, *Bulletin of the American Meteorological Society*, 79, 61  
 Torres D. F., Rea N., Esposito P., Li J., Chen Y., Zhang S., 2012, *ApJ*, 744, 106  
 Valtaoja E., Terasranta H., Urpo S., Nesterov N. S., Lainela M., Valtonen M., 1992, *A&A*, 254, 71  
 Van der Laan H., 1966, *Nature*, 211, 1131  
 Zimmermann L., Fuhrmann L., Massi M., 2015, *A&A*, 580, L2

This paper has been typeset from a  $\text{\LaTeX}$  file prepared by the author.